

Finite Element Solution of a Converging Hydrodynamic Flow-Field between Stationary Porous and Sliding Nonporous Surfaces

M. MALIK

Reader in Mechanical Engineering, University of Roorkee, India

and

R. SINHASAN

Associate Professor in Mechanical Engineering, University of Roorkee, India

SUMMARY The converging hydrodynamic flow-field between stationary porous and sliding nonporous surfaces has been analysed by finite element method. The analysis also takes into account tangential velocity slip at the interface of fluid film and porous matrix. The computed results which include pressure distribution, load support, and friction force at moving surface are for two types of sliders. The results illustrate fully the effect of porosity and tangential velocity slip on the performance characteristics of the sliders.

1 INTRODUCTION

The analysis of converging hydrodynamic flow-field of slider bearings, in which one surface is stationary and the other is sliding, has conventionally been the basis of all studies in hydrodynamic lubrication. A slider provides geometrically and analysis wise simplest bearing configuration, yet its analysis reveals the effect of all parameters under investigation on the performance of hydrodynamic bearings. This paper presents the analysis of the slider bearing in which the stationary surface is porous. The flow conditions have been assumed to be incompressible laminar and isothermal and the lubricant to be Newtonian. The flow-field in the clearance space of the slider is governed by a modified form of Reynolds equation (Prakash and Vij, 1974) which takes into account the flow of lubricant from and into the porous matrix and also the tangential velocity slip at the interface of the fluid film and porous matrix in accordance with Beavers-Joseph criterion (1967). This modified Reynolds equation is coupled to the Laplace equation which governs the pressure distribution in the porous matrix. In the present paper the solution of fluid film and porous matrix flow fields has been obtained by finite element method. The finite element method has the advantage of not only tackling complex geometrical boundaries of the field domain, but also of handling the boundary conditions properly. Although finite element method has now become quite popular among lubrication engineers, it has not received their due attention for the application of the method to porous bearing lubrication problems. The authors have come across only one reference (Eidelberg and Booker, 1976) in the published literature which only demonstrates the application of finite element method to porous bearing lubrication problem. No practical bearing configuration has however been analysed in this work. The aim of the present work is to investigate the effect of tangential velocity slip on the slider bearing performance. Two types of sliders, namely, plane inclined slider and Rayleigh step slider, have been considered

for this investigation. The computed results presented in graphical form include pressure distribution, load support, and friction force at moving surface. It has been concluded that inclusion of slip always results in decrease in both the load support and the friction force at the moving surface.

2 NOTATION

- B = length of slider in x-direction (m)
 h_1 = inlet film thickness (m)
 p, p^* = pressure (N/m^2)
 P, P^* = nondimensional pressure, $p/(\mu UB/h_1^2)$, $p^*/(\mu UB/h_1^2)$
U = velocity of sliding surface (m/s)
 λ = aspect ratio, (bearing length in y-direction)/B
 μ = absolute viscosity (Ns/m^2)
 Φ = permeability parameter, $\Phi_p B/h_1^3$
 Φ_p = porosity (m^2)

3 ANALYSIS

3.1 Field Equations

The coordinate system and geometries of the plane inclined slider and Rayleigh step slider are shown in Fig.1.

The fluid film pressure in the clearance space of stationary porous and sliding nonporous surfaces, is governed by the following Reynolds equation (Prakash and Vij, 1974)

$$\frac{\partial}{\partial x} \left[\frac{H^3}{12} (1 + \epsilon_1) \frac{\partial P}{\partial x} \right] + \frac{\partial}{\partial y} \left[\frac{H^3}{12} (1 + \epsilon_1) \frac{\partial P}{\partial y} \right] - \Phi \frac{\partial P^*}{\partial z} \Big|_{z=H_B} = \frac{1}{2} \frac{\partial}{\partial x} [H(1 + \epsilon_0)] \quad (1)$$

where

$$\epsilon_0 = \frac{S}{S+H}, \quad \epsilon_1 = \frac{3(2\alpha^2 S^2 + SH)}{H(S+H)}, \quad S = \frac{1}{\alpha} \sqrt{\frac{h_1}{B}} \quad (2)$$

The function ϵ_0 and ϵ_1 depend on the porosity of the slider (Φ), slip coefficient (α) and the slider and film geometry (h_1/B and

H). These functions account for tangential velocity slip in accordance with Bearers-Joseph criterion(1967).

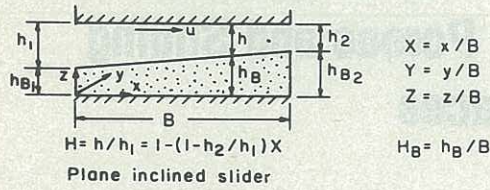


Figure 1 Geometry of porous sliders

The nondimensional unit slot flow rates in the fluid film are given by

$$Q_x = \int \left[-\frac{H^3}{12}(1+\epsilon_1) \frac{\partial P}{\partial X} + \frac{H}{2}(1+\epsilon_0) \right] dY \quad (3)$$

$$Q_y = \int \left[-\frac{H^3}{12}(1+\epsilon_1) \frac{\partial P}{\partial Y} \right] dX$$

The pressure distribution in a porous medium of uniform isotropic porosity is governed by the following Laplace equation

$$\frac{\partial^2 P^*}{\partial X^2} + \frac{\partial^2 P^*}{\partial Y^2} + \frac{\partial^2 P^*}{\partial Z^2} = 0 \quad (4)$$

The nondimensional unit flow rates in the porous matrix are given by

$$Q_x^* = -\Phi \iint \frac{\partial P^*}{\partial X} dY dZ$$

$$Q_y^* = -\Phi \iint \frac{\partial P^*}{\partial Y} dX dZ \quad (5)$$

$$Q_z^* = -\Phi \iint \frac{\partial P^*}{\partial Z} dX dY$$

where the above expressions follow from Darcy's law.

3.2 Finite Element Formulation

The clearance space film pressure (P) is a function of coordinates X and Y while pressure in porous matrix (P*) is a function of X, Y and Z coordinates. The flow-field for the clearance space is therefore discretized into isoparametric four-noded rectangular elements and that of porous matrix into isoparametric eight-noded hexahedral elements. The variation of pressure over these elements is expressed as

$$P_e = \sum_{j=1}^4 N_j P_j$$

$$P_e^* = \sum_{j=1}^8 N_j^* P_j^* \quad (6)$$

where e designates an element. N_j and N_j^* are shape functions for four-noded rectangular and eight-noded hexahedral elements respectively (Heubner, 1975). P_j and P_j^* are nodal pressures.

Following the Galerkin's method(Heubner,

1975), the element field equations may be written as

$$\iint_{A^e} \left\{ \frac{\partial}{\partial X} \left[\frac{H^3}{12}(1+\epsilon_1) \frac{\partial P^e}{\partial X} \right] + \frac{\partial}{\partial Y} \left[\frac{H^3}{12}(1+\epsilon_1) \frac{\partial P^e}{\partial Y} \right] - \Phi \frac{\partial P^e}{\partial Z} \right\} N_1 dA^e = 0 \quad (7)$$

for the Reynolds equation, and

$$\iiint_{V^e} \left(\frac{\partial^2 P^e}{\partial X^2} + \frac{\partial^2 P^e}{\partial Y^2} + \frac{\partial^2 P^e}{\partial Z^2} \right) N_1^* dV^e = 0 \quad (8)$$

for the Laplace equation.

In the above equations A^e and V^e represent the area and volume elements, respectively, of the discretized domains.

After substituting Equations(6) in Equations (7) and (8) and simplifying, following element equations are obtained.

$$[F_e] \{P_e\} = \{H_{se}\} - \{Q_e\} \quad (9)$$

(4x4) (4x1) (4x1) (4x1)

$$[F_e^*] \{P_e^*\} = -\{Q_e^*\} \quad (10)$$

(8x8) (8x1) (8x1)

where

$$F_{e,ij} = \iint_{A^e} \left[\frac{H^3}{12}(1+\epsilon_1) \left(\frac{\partial N_i}{\partial X} \frac{\partial N_j}{\partial X} + \frac{\partial N_i}{\partial Y} \frac{\partial N_j}{\partial Y} \right) + \Phi N_i \frac{\partial N_j}{\partial Z} \right] dX dY$$

$$H_{se,i} = \frac{1}{2} \iint_{A^e} H(1+\epsilon_0) \frac{\partial N_i}{\partial X} dX dY$$

$$Q_{e,i} = \int Q_x N_i dY + \int Q_y N_i dX$$

$$F_{e,mn}^* = \Phi \iiint_{V^e} \left(\frac{\partial N_m^*}{\partial X} \frac{\partial N_n^*}{\partial X} + \frac{\partial N_m^*}{\partial Y} \frac{\partial N_n^*}{\partial Y} + \frac{\partial N_m^*}{\partial Z} \frac{\partial N_n^*}{\partial Z} \right) dX dY dZ$$

$$Q_{e,m}^* = \iint Q_x^* N_m^* dY dZ + \iint Q_y^* N_m^* dX dZ + \iint Q_z^* N_m^* dX dY$$

$i, j = 1, 2, 3, 4$ and $m, n = 1, 2, \dots, 8$.

Using the usual assembly procedure of finite element method, the element wise contributions of Eqs.(9) and (10) result in following global equations for the entire domains of the field variables.

$$[F] \{P\} = \{H_s\} - \{Q\} \quad (11)$$

$$[F^*] \{P^*\} = -\{Q^*\} \quad (12)$$

3.3 Solution Method

It is obvious that at the interface ($Z=H_B$) of the fluid film and porous matrix, the two flow-fields have common nodes and would have common pressure at these nodes so that the pressures of the two flow-fields match at the interface. Thus, Equation (11) can be merged with Equation (12), so that the elements of Equations (11) and (12) corresponding to the common nodes are algebraically added.

The boundary conditions of two flow-fields are:

(i) Pressure at the surface $X=0, X=1, Y=0$

and $Y=\lambda$ is zero.

- (11) Flow at all internal nodes and across the surface $Z=0$ is zero.

The number of unknowns are as many as the number of equations, since at a particular node either pressure or flow is known. The unknown pressures and flows may thus be obtained via linear simultaneous equations (11) and (12).

2.4 Load Support and Friction

The nondimensional load support of the slider is given by

$$W = \sum_{e=1}^{N_f} \iint_{A_e} P_e dX dY \quad (13)$$

where N_f denotes the number of rectangular elements at the interface.

The nondimensional friction force at the sliding surface is given by (Cusano, 1979)

$$F = \sum_{e=1}^{N_f} \iint_{A_e} \left[\frac{1}{2} \frac{\partial P}{\partial X} e^{H(1 + \frac{1}{3}\xi_1) + \frac{1}{H}(1 - \xi_0)} \right] dX dY \quad (14)$$

4 RESULTS AND DISCUSSION

The geometrical data of the two sliders analysed in this work are as follows

$$\lambda = 1.0, h_1/h_2 = 2.0, h_{B1}/B = 0.2 \\ B_1/B = 0.5 \text{ (for step slider)}$$

The porosity of the porous matrix is accounted by the permeability parameter Φ . The tangential velocity is characterized by slip coefficient α and its value depends on the porous material. For laminar channel flow, the value of α estimated by Beavers, Sparrow and Magnuson (1970) is approximately 0.1 and the same value has been adopted here. The function ξ_1 and ξ_0 accounting for velocity slip, also involve Φ and B/h_1 ratio. For a detailed study of the effects of slip, the following ranges of Φ and B/h_1 ratio have been chosen

$$\Phi = 0.0, 0.001, 0.005, 0.01, 0.05, 0.1 \text{ and } 0.5 \\ B/h_1 = 500, 750, 1000, 1250 \text{ and } 1500,$$

where $\Phi = 0.0$ refers to the nonporous slider. For a porous slider in which slip is disregarded, ξ_0 and ξ_1 are zero.

The computed results of present investigation are given in the graphical form in Figures 2 through 7. The pressure distributions (Figures 2 and 3) are plotted on the mid-plane $Y=\lambda/2$ as pressures in Y -direction are symmetrical about this plane. The results are given here in a manner to show a comparison of the slider performance characteristics (pressure distribution, load support and friction force) for three cases of stationary surface, namely, nonporous, porous without slip and porous with slip. It is seen that pressure and load support decrease with increase in permeability and further reduction results by inclusion of slip. The effect of slip on pressure and load support seems to be most pronounced for $\Phi = 0.01$ and on either

side of permeability range, the effect of slip tends to decrease. In fact, for $\Phi=0.5$, the load support curves for without and with slip condition overlap each other.

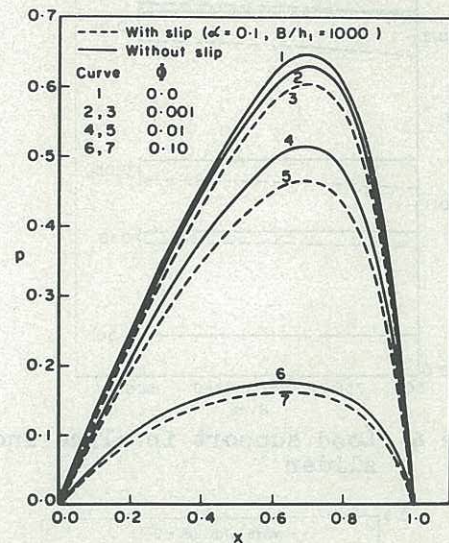


Figure 2 Mid-plane pressure distribution in plane inclined slider

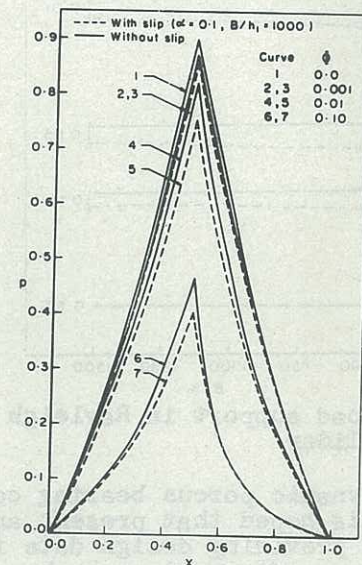


Figure 3 Mid-plane pressure distribution in Rayleigh step slider

The friction forces for nonporous and porous without slip cases are almost the same. However friction force decreases with the inclusion of slip. Unlike pressure distribution and load support, the effect of slip on friction force increases with permeability.

It may be seen from Equations (2) that ξ_0 and ξ_1 decrease with increase in B/h_1 ratio. Thus it is also seen from all the performance characteristics curves that slip effects decrease with increase in B/h_1 ratio.

5 CLOSURE

The finite element analysis of the porous slider presented in this paper is entirely general and can be conveniently applied

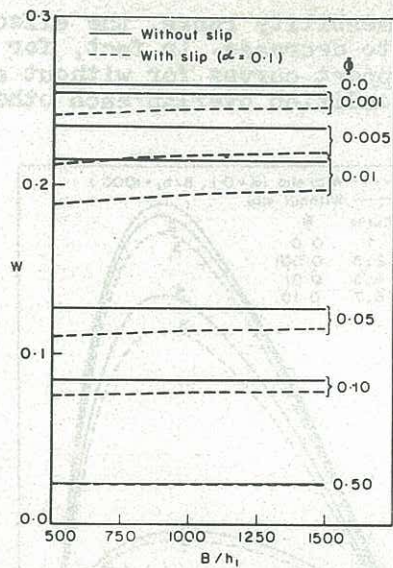


Figure 4 Load support in plane inclined slider

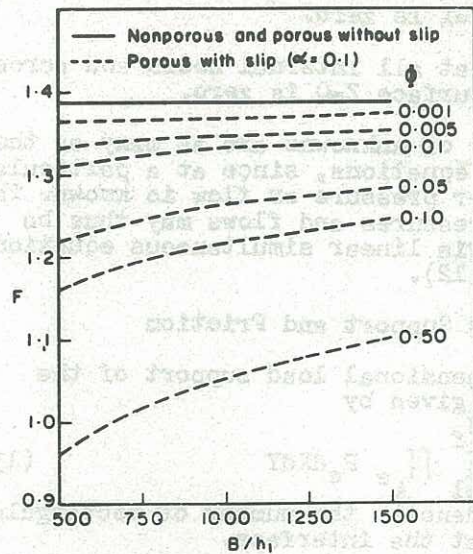


Figure 6 Friction force in plane inclined slider

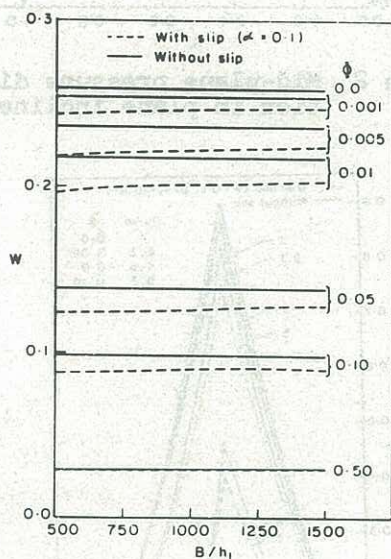


Figure 5 Load support in Rayleigh step slider

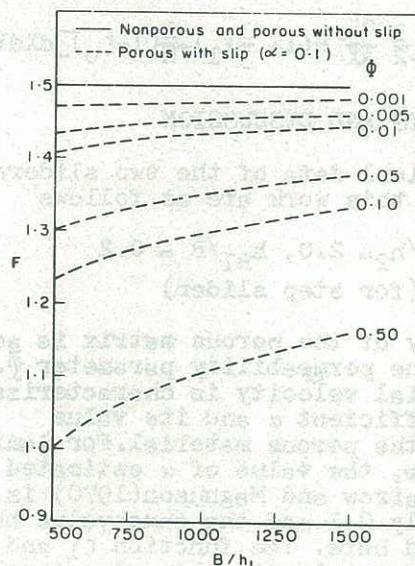


Figure 7 Friction force in Rayleigh step slider

to any hydrodynamic porous bearing configuration. It is hoped that present analysis would help in providing design data for porous bearing configurations such as sector shaped thrust and grooved journal bearings.

6 REFERENCES

- BEAVERS, G.S. and JOSEPH, D.D.(1967). Boundary conditions of a naturally permeable wall. Trans.J.of Fluid Mech. Vol.30, pp.197-207.
- BEAVERS, G.S., SPARROW, E.M. and MAGNUSON, R.A.(1970). Experiments on coupled parallel flows in a channel and a bounding porous medium. Trans.ASME,J. of Basic Engg. Vol.92, pp.843-848.

CUSANO, C.(1979). An analytical study of starved porous bearings. Trans.ASME,J.of Lub.Tech. Vol.101,pp.38-47.

EIDELBERG, B.E. and BOOKER, J.F.(1976). Application of finite element methods to lubrication: Squeeze film between porous surfaces. Trans.ASME, J.of Lub.Tech. Vol.98,pp.175-180.

HUEBNER, K.H.(1975). The finite element method for engineers, New York, John Wiley and Sons.

PRAKASH, J. and VIJ, S.K.(1974). Analysis of narrow porous journal bearing using Beavers-Joseph criterion of velocity slip. Trans. ASME, J.of Lub.Tech. Vol.96, pp.348-354.